

Study of the Finite Density State based on SU(2) Lattice QCD

Shin Muroya^a, Atsushi Nakamura^b and Chiho Nonaka^{c*}

^aTokuyama Women's Coll. Tokuyama, 745-8511, Japan

^bIMC, Hiroshima University, Higashi-Hiroshima 739-8521, Japan

^cRadiation Lab, RIKEN, 2-1 Hirosawa, Wako, Saitama, 351-0198, Japan

We report our recent numerical studies on two-color QCD with Wilson fermions. First the phase structure of the system in (κ, μ) -plane is analyzed by measuring Polyakov line, baryon number density, gluon energy density and Polyakov line susceptibility. Then meson and baryon (di-quark) propagators are investigated. We find that the vector meson mass decreases near μ_c . This phenomena can be related to the low-mass lepton-pair enhancement observed in CERES experiment. Since our lattice is small, in order to confirm the results, we calculate both periodic and anti-periodic boundary condition cases. Preliminary calculations of color averaged, symmetric and anti-symmetric forces of qq system obtained from Polyakov line correlations, and gluon propagators are reported.

1. Introduction

Finite density QCD has attracted much attention recently: we are expecting that QCD has a rich structure when we add a density or chemical potential axis in parameter space. The finite temperature deconfinement transition line starts at $\mu = 0$, which might be a cross-over accompanied by a tri-critical point at finite μ . At high μ and relatively low temperature, there would be a new form of matter such as color superconductive phase, or color-flavor locking phase, which are speculated by mainly perturbative calculations [1].

Non-perturbative study of the finite density QCD by lattice simulations is highly required, but because of the famous difficulty, the direct Monte Carlo simulation of SU(3) system is very difficult. Many approaches have been reported, [2–6], and yet, no reliable algorithm is known to investigate color SU(3) QCD at low temperature with large chemical potential. Color-SU(2) is currently the unique model by which we can study these regions non-perturbatively. After the first trial of the calculation[7], there had been no work during many years. Because of the recent rapid progress of theoretical understanding of the system [8,9], however, the calculation has been activated [10–

12].

In this report, we study the finite density QCD by Wilson fermions. We investigate the phase structure in (κ, μ) -plane for Iwasaki improved-gauge action. In order to take account of the fermion determinant, we use an algorithm in which the ratio of the determinant is evaluated explicitly at each Metropolis update process [13].

2. Phase Structure

In Fig.1, we show the average of Polyakov line in (κ, μ) -plane at $\beta = 0.7$. We evaluate also baryon number density, gluon energy density and Polyakov line susceptibility, and especially from the peak of the Polyakov line susceptibility we can determine the confinement/deconfinement phase transition regions. In both boundary conditions², the behaviors of these quantities are essentially the same [13].

We study several cases by varying lattice size (4^4 , $4^3 \times 8$, $4^3 \times 12$), the boundary conditions and the number of flavor ($N_f = 2, 3$).

Calculations become unstable and break down at large chemical potential regions[13]. In such cases, negative determinant appears for $N_f = 3$.

*Presenter

²Periodic (anti-periodic) refers the periodic (anti-periodic) boundary condition for quark fields in spatial directions.

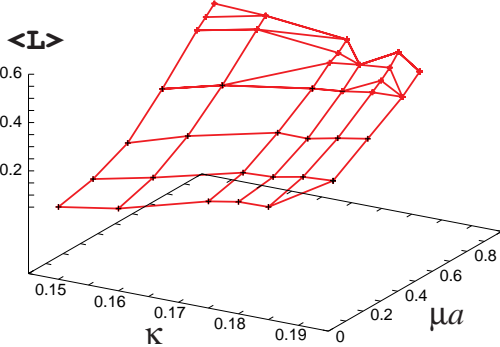


Figure 1. Behavior of Polyakov line in (κ, μ) -space.

3. Meson and diquark propagators

We calculate meson and di-quark propagators in pseudo-scalar and vector channels. We find that ρ meson mass drops as μ reaches to the critical region. In order to confirm this unexpected result, we calculate both periodic and anti-periodic boundary conditions and several κ 's ($\kappa = 0.150, 0.160, 0.175$). In Fig.2 we show π and ρ masses as a function of μ for $\kappa = 0.160$ (periodic boundary condition). Although our statistic is not enough to extrapolate them to the chiral limit, the signal of the anomalous behavior of the vector channel is clearly seen.

At $\mu = 0$, because of the QCD inequality [9], the pseudo-scalar channel has the lightest mass, but there is no such a condition for the finite density state. Indeed there are several conjectures in literatures [14]. If our result shown in Fig.2 is not a special feature of the color SU(2) model, this is the first lattice observation of the drop of the vector meson mass which may play an important role in the phenomenological analyses on large low-mass lepton-pair enhancement measured in CERES [15].

Another possibility is that the vector meson channel is mixed with the vector diquark one, $\psi^c \gamma_5 \gamma_\mu \psi$, at high μ and their masses are distorted³. In this case, we can study “meson” and “diquark” mixing in color SU(2) QCD.

³We thank Thomas Schaefer for useful discussions on $\bar{\psi} \gamma_\mu \psi / \psi^c \gamma_5 \gamma_\mu \psi$ mixing.

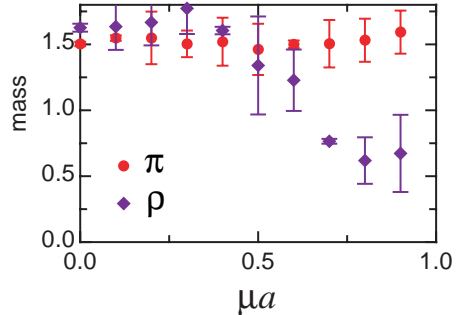


Figure 2. π and ρ masses as a function of μ for $\kappa = 0.160$ with periodic boundary condition

4. Force between $qq / \bar{q}q$

In the previous section, we show that the vector meson may have a peculiar behavior at finite density. Above μ_c at low temperature, the condensation of qq may occur. We need tools to understand the vacuum structure numerically.

From Polyakov line correlations, color average heavy quark potential is calculated. One can also obtain color singlet (V_1) and triplet potential (V_3) for $q\bar{q}$ system: $N_c \times \bar{N}_c = 1 \oplus (N_c^2 - 1)$ [16]. Color symmetric (V_s) and anti-symmetric (V_a) potential for qq system can be also evaluated: $N_c \times N_c = \frac{1}{2}N_c(N_c + 1) \oplus \frac{1}{2}N_c(N_c - 1)$. In color SU(2), $V_1 = V_a$ and $V_3 = V_s$ even at $\mu \neq 0$. Therefore if there would exist difference between qq and $q\bar{q}$ states, it should originate in Dirac structure.

In Fig.3, we plot preliminary data of color singlet potential. The rotational invariance is good by virtue of the renormalization group improved gauge action. The singlet (triplet) potential is attractive (repulsive) and the forces become weaker as μ increases. We fix the gauge in Lorentz gauge for the color-dependent force and gluon propagators discussed in the following.

We study gluon propagators as a tool to investigate the finite density QCD,

$$G_{\mu\nu}(P_0, P_x, P_y, z) = \langle \text{Tr} A_\mu(P_0, P_x, P_y, z) \times A_\nu(-P_0, -P_x, -P_y, 0) \rangle. \quad (1)$$

We set the momenta as $(P_0, P_x, P_y) =$

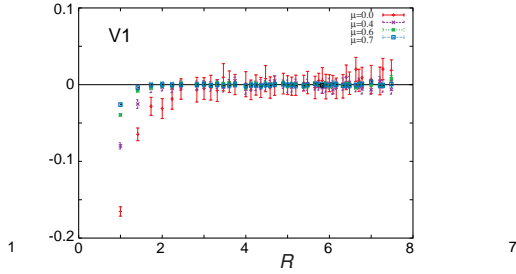


Figure 3. Color singlet potential V_1 for $\mu = 0.0, 0.4, 0.6$ and 0.7 .

$(0, 2\pi/N_x, 0)$. The electric and magnetic parts of the propagator, $G_e = G_{tt}$ and $G_m = G_{yy}$, are expected to behave as, $G_{e(m)}(z) \propto \exp(-E_{e(m)}z)$. When the system is screened at the finite temperature and/or finite density, the screening effects should appear as $E_e = \sqrt{(P_x^2 + M_e^2)}$ and $E_m = \sqrt{(P_x^2 + M_m^2)}$, with M_e and M_m being electric and magnetic masses of the gluons, respectively. At $T = 0$ and $\mu = 0$ the screening is infinite and the propagators vanish at long distance [17].

We show in Fig.4 a preliminary result for $G_m(z)$. As μ increases, the screening becomes weaker, i.e., the system shows the deconfinement feature, but at $\mu = 0.7$ the propagator at long range seems to drop. It is an urgent future task to confirm the phenomena, because it could be an indication of a new phase at large μ .

Acknowledgment This work is partially supported by Grant-in-Aide for Scientific Research by Monbu-Kagaku-sho (No.11440080 and No. 12554008) and ERI of Tokuyama Univ. Simulations were performed on SR8000 at IMC, Hiroshima Univ., SX5 at RCNP, Osaka Univ., SR8000 at KEK and VPP5000 at Science Information Processing Center, Tsukuba Univ.

REFERENCES

1. K. Rajagopal and F. Wilczek, [hep-ph/0011333](#).
2. J. Engels, et al., Nucl. Phys. B558 (1999) 307.
3. S. Choe et al., Phys. Rev. D63 (2001) 054501.
4. Z. Fodor and S. D. Katz, JHEP 0203 (2002)

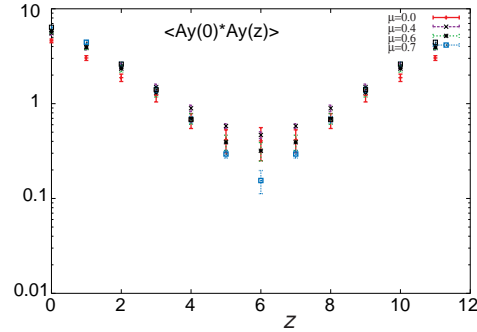


Figure 4. Transverse gluon propagator for different μ . Lattice size is $8 \times 4 \times 12 \times 4$.

- 014.
5. C.R. Allton et al., [hep-lat/0204010](#).
6. Ph. de Forcrand and O. Philipsen, [hep-lat/0205016](#); M. D'Elia and M.P. Lombardo, [hep-lat/0205022](#).
7. A. Nakamura, Phys. Lett. 149B (1984) 391.
8. J. B. Kogut et al., Nucl. Phys. B582 (2000) 477.
9. J. B. Kogut, M. A. Stephanov and D. Toublan, Phys. Lett. B464 (1999) 183.
10. M.-P. Lombardo, [hep-lat/9907025](#).
11. S. Hands et al., Nucl. Phys. B558 (1999) 327.
12. S. Morrison and S. Hands, [hep-lat/9902012](#).
13. S. Muroya, A. Nakamura and C. Nonaka, Nucl. Phys. B Proc. Suppl. 94 (2001) 469; *ibid.*, Nucl. Phys. B Proc. Suppl. 106 (2002) 453.
14. G. E. Brown and M. Rho, Phys. Rev. Lett. (1991) 2720; T. Hatsuda and S. H. Lee, Phys. Rev. C46 (1992) R34; M. Harada et al. [hep-ph/0111120](#); Yokokawa et al. [hep-ph/0204163](#).
15. H. Appelshaeuser, talk at "Compressed Baryonic Matter Workshop, 2002" <http://www.gsi.de/cbm2002/transparencies/happelshaeuser1/index.html>; R. Rapp and J. Wambach, Adv.Nucl.Phys. 25 (2000).
16. S. Nadkarni, Phys. Rev. D34 (1986) 3904.
17. A. Nakamura, Prog.Theor.Physics, Suppl.131 (1998) 585.